J. Physiol. (1984), **347**, *pp.* 751–768
With 1 plate and 8 text-figures
Printed in Great Britain

VOLTAGE CLAMP OF RAT AND HUMAN SKELETAL MUSCLE: MEASUREMENTS WITH AN IMPROVED LOOSE-PATCH TECHNIQUE

BY W. ALMERS, W. M. ROBERTS AND R. L. RUFF

From the Department of Physiology and Biophysics, SJ-40, University of Washington, Seattle, WA 98195, U.S.A.

(*Received 21 June 1983*)

SUMMARY

1. Intact fibres of human intercostal and rat omohyoid muscles were studied at 23 °C with a loose-patch voltage-clamp technique that employed two concentric micropipettes to electrically isolate small-diameter (10–15 μm) patches of sarcolemma. This method allows investigation of membrane excitability under highly physiological conditions.

2. Step depolarizations to 0 mV elicited sodium inward currents that reached peak values of up to 20 mA/cm^2 within 250 μs, and then declined. In human muscle, the reversal potential ($\tilde{E}_{Na}$) was $\sim$ 40 mV, and maximal conductances ($\tilde{G}_{Na}$) ranged from 44 to 360 mS/cm^2. In rat muscle, $\tilde{E}_{Na}$ was 42 mV and $\tilde{G}_{Na}$ ranged from 100 to 250 mS/cm^2. Sodium channels in rat and human muscle were indistinguishable in most aspects of their kinetic behaviour and voltage dependence.

3. Outward potassium currents were small by comparison (usually < 2 mA/cm^2) and saturated at positive potentials. The maximum potassium conductance ($\tilde{G}_K$) ranged from 0 to 19 mS/cm^2 (human) and from 4 to 12 mS/cm^2 (rat muscle).

INTRODUCTION

The most definitive information about impulse generation in excitable cells has been obtained with voltage-clamp methods. In frog skeletal muscle extensive information has been obtained with the 'three micro-electrode' (Adrian, Chandler & Hodgkin, 1970), sucrose-gap (Ildefonse & Rougier, 1972) and Vaseline-gap techniques (Hille & Campbell, 1976). More recently, these methods have also been applied successfully to rat skeletal muscle (Adrian & Marshall, 1977; Duval & Léoty, 1978; Pappone, 1980). By contrast, voltage-clamp data on human skeletal muscle are scant (De Doursey, Bryant & Lipicky, 1982; Lehmann-Horn, Rüdel, Ricker, Lorković, Dengler & Hopf, 1983) and our views on electrical excitability of human muscle are largely an extrapolation of data obtained from frog and, to a lesser extent, from rat muscle. Electrical studies on human skeletal muscle are of interest because cell membrane aberrations may contribute to certain disease states, such as the various periodic paralyses (Lehmann-Horn *et al.* 1983; for a recent review see Ruff & Gordon, 1984), and the several kinds of myotonic disorders (e.g. Lipicky & Bryant, 1973; Lehmann-Horn, Rüdel, Dengler, Lorković, Haass & Ricker, 1981).

Systematic biophysical investigations of human skeletal muscle are often limited by the availability of suitable biopsy material. One therefore requires a voltage-clamp method that is convenient, allows data collection with a high success rate, and permits experimentation under conditions that are as physiological as possible. The 'loose-patch' voltage-clamp technique (Stühmer & Almers, 1982; Almers, Stanfield & Stühmer, 1983*a*) has many features that are consistent with these requirements. Here we use an improved 'loose-patch' technique to study and compare sodium and potassium currents in rat and normal human skeletal muscle. Our results show that loose-patch methods may prove useful in electrophysiological studies of normal and diseased human muscle.

METHODS

External intercostal muscles were obtained with the informed consent of four patients (aged 28–45 years) undergoing surgery for reasons unrelated to muscle disease or to this study. On physical examination, they showed no sign of weakness or respiratory difficulty, and there was no family medical history of muscle disease. Consequently we consider that our data pertain to normal human muscle. Before surgery, general anaesthesia was induced with pentobarbitol (100 mg intraveneously) and maintained by inhalation of a mixture of 34% O_2, 65% N_2O and 1% halothane. Local anaesthetics or neuromuscular blocking agents were not used, and electrocautery was not used at the biopsy site. Once removed the muscle specimen was immediately placed in Tyrode solution (composition (mM, 23 °C): NaCl, 120; KCl, 4·5; $NaHCO_3$, 25; NaH_2PO_4, 1; $MgCl_2$, 1; $CaCl_2$, 2; glucose, 12) and gassed vigorously with 95% O_2/5% CO_2. The pH of the gassed solutions was 7·5. The muscle was then transported to the laboratory where individual fascicles were dissected free. The time between excision of the biopsy and the beginning of electrophysiological experiments is estimated as 4–8 h; throughout that time the muscle was kept in Tyrode solution at room temperature. For studies of rat muscle the omohyoid, a fast-twitch neck muscle, was removed from 300–320 g male Sprague–Dawley rats as described previously (Ruff, Martyn & Gordon, 1982). For both human and rat muscle the surface connective tissue was dissected away, and enzyme treatment was avoided. The experiments were performed at 23 ± 1 °C. In all except a few early experiments on human muscle, the small (2 ml) experimental chamber was continuously perfused (3 ml/min) with gassed Tyrode solution.

We used a modified version of the 'loose-patch' voltage-clamp method described earlier (Almers *et al.* 1983*a*; Stühmer, Roberts & Almers, 1983). The new version employed a concentric arrangement of two glass micropipettes as shown in Pl. 1 and Fig. 1, and may be compared to a concentric sucrose-gap method developed by Henćek, Nonner & Stämpfli (1969). The concentric pipettes were pulled from glass capillaries which had an inner tube held in the centre of an outer tube by three equally spaced support tubes. When pushed against the cell surface, the outer pipette wall electrically isolates a membrane patch which is subdivided by the inner barrel wall into a central region and a surrounding annulus. The voltage-clamp amplifier, which is an elaboration of the circuit used for single-barrelled pipettes (Stühmer *et al.* 1983), holds both the centre and surround at the command potential. Details of electrode fabrication and voltage-clamp circuit will be provided elsewhere (W. M. Roberts & W. Almers, unpublished).

The current monitor is connected to the inner barrel and records current crossing the central membrane patch only, plus some current across the small area of membrane in contact with the tip of the central pipette. Since all of this membrane experiences a potential nearly equal to the command potential, the rim effects observed with single-barrelled electrodes (Almers *et al.* 1983*a*) are greatly reduced. Patch currents were converted to current densities by dividing by the area of the centre barrel tip, as measured from end-on photographs. The six electrodes used here collected current from areas ranging from 95 to 154 μm^2. These values do not include the small area beneath the rim of the central pipette, so we may underestimate slightly the membrane area from which current was collected. The membrane area enclosed by the outer pipette was 3–4 times the centre area.

Four resistances are important in determining stability and noise in these recordings (Fig. 1) and

were measured for each patch. Average values (mean ± S.D., kΩ) were: R_{ip}, 422 ± 64; R_{op}, 243 ± 31; R_{is}, 591 ± 271; R_{os}, 448 ± 171. R_{ip} was measured every time before a new patch was approached. R_{is} and R_{os} were measured after making the seal and applying suction to the outer barrel. The previously measured value of R_{ip} was then entered on a calibrated potentiometer that determined the magnitude of the series resistance compensated by our circuit. The outer barrel series resistance

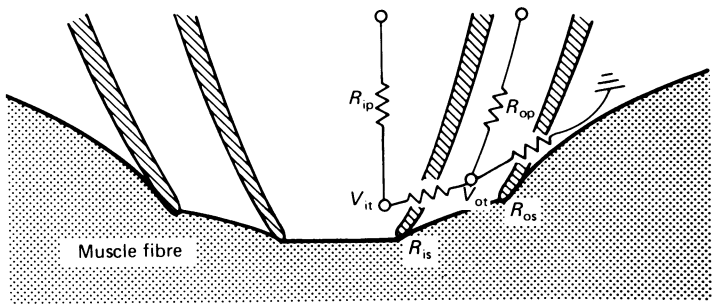

Fig. 1. Idealized representation of the patch electrode in contact with a muscle fibre showing the resistances of the inner pipette (R_{ip}), outer pipette (R_{op}), inner seal (R_{is}) and outer seal (R_{os}). The voltage clamp holds the voltages V_{it} and V_{ot} equal to the command voltage.

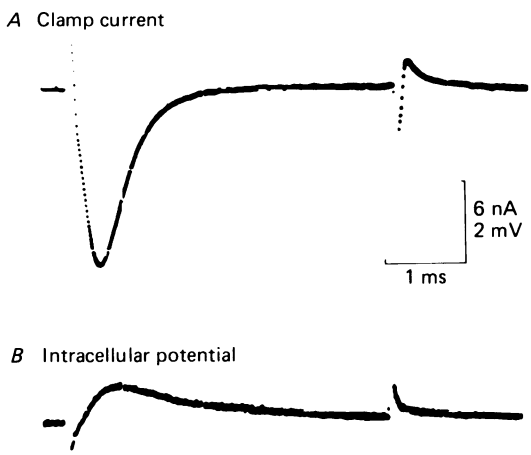

Fig. 2. *A*, current through a membrane patch recorded during a 4 ms duration step depolarization from the holding potential (h.p. = −108 mV) to E = −23 mV. This step amplitude elicited the largest sodium current (11 nA) seen in this patch. The fast transient currents at the step edges are due to stray capacitances in the electronics and patch electrode; they were removed from all other current traces by the digital subtraction procedure described in the text. *B*, intracellular potential (E_0) recorded at the same time with a glass micro-electrode, showing less than 1 mV perturbation. The voltage transients seen at the step edges are predominantly due to capacitive coupling between intracellular and patch electrodes. Fibre H-2; area = 95 μm^2; R_{is} = 1·03 MΩ; R_{os} = 0·32 MΩ; T = 23 °C.

compensation was adjusted until small command steps caused only transient current through the centre barrel that arose from stray capacitances in the system, varied linearly with voltage and were reduced as much as possible by analogue subtraction. After this was done, step depolarizations of sufficient amplitude produced currents as in Fig. 2*A*. These currents were passed through a four-pole Bessel low-pass filter with corner frequency of 8 kHz and then digitized at 50 kHz sampling rate and 12 bit resolution.

Any residual components of current varying linearly with potential (e.g. the rapid transients at beginning and end of the depolarizing pulse in Fig. 2*A*) were removed digitally by point-for-point subtraction of two current traces. One contained the mixture of active current and capacitive or leakage components (e.g. as in Fig. 2*A*), the other an appropriately scaled and signal-averaged version of leakage and capacitive currents during steps at potentials too negative to elicit active currents. The pulse protocol used was similar to that of Almers *et al.* (1983*a*) except that no hyperpolarizing prepulse was given.

The unfiltered patch current monitor responded with a time constant of 30 μs when 40 nA current steps were applied to the centre of a simulated patch using a network of resistors and capacitors to mimic the electrode and seal impedances. In experiments on rat or human muscle, the half-response time of the voltage clamp and current monitor to step changes in the command potential was inferred from the time course with which potassium outward current (see later) disappeared at the end of a large depolarizing pulse lasting 4 ms. Averaging all records from human fibres showing late outward currents larger than 0·5 nA gave a half-response time of 34 μs in addition to the 48 μs delay introduced by the Bessel filter.

Most fibres were impaled with an intracellular electrode (3 M-potassium chloride, 10–50 MΩ) at a distance of 100–150 μm from the patch electrode after a set of patch recordings was completed. Since we did not control the intracellular potential in these experiments, we needed to verify that membrane currents evoked by the patch pipette did not cause significant variations from the resting level. Fig. 2*B* shows that a typical 11 nA sodium current caused an intracellular potential change of 1 mV.

RESULTS

Membrane currents in human muscle

Data were collected from seventeen fibres from four biopsies. By the time the biopsies had been installed in our experimental set-up and were ready for electrophysiological recording, resting membrane potentials measured with intracellular microelectrodes ranged from −48 to −73 mV (mean ± S.E. of mean, $-63 \pm 3{\cdot}6$ mV, $n = 6$). At these membrane potentials the fibres were probably inexcitable, because no, or only small, active currents could be recorded from them with our concentric electrodes. However, large active currents could always be restored within ~ 10 min by applying a steady 20–40 mV hyperpolarizing potential to the patch and removing slow inactivation (Almers, Stanfield & Stühmer, 1983*b*). Fig. 3 was obtained in this way and panels *A* and *C* show superimposed current traces recorded during 4 ms long test depolarizations of 45–180 mV amplitudes. Results from two fibres are included. Patch membrane depolarization elicits currents that rise to a peak and then decline; these currents are inward for most test depolarizations, but show a clear reversal when depolarization exceeds 130–150 mV in amplitude. They are abolished by tetrodotoxin, the half-blockage concentration being about 20 nM (13 °C, one experiment with the Vaseline-gap technique: E. W. McCleskey, R. L. Ruff & W. Almers, unpublished). Voltage dependence and kinetics of these currents are closely similar to those observed for sodium channels of rat skeletal muscle (Pappone, 1980: see later), and therefore we believe these currents to flow through voltage-sensitive sodium channels.

The currents in Fig. 3*A* are about fourfold larger than those in Fig. 3*C*, but the two sets of traces are similar or identical in kinetics and voltage dependence (see later, e.g. by comparing open and filled symbols in Fig. 5). The smaller currents in Fig. 3*C* and *D* cannot be due to an inferior seal, since seal resistances were actually larger than in Fig. 3*A* and *B*. Evidently, functional sodium channels occurred at different densities in the two cases. Peak sodium current densities varied over a nearly tenfold

range from fibre to fibre. Fig. 3*A* and *B* show the largest currents recorded in this work, while Fig. 3C and *D* are from a fibre with relatively small currents.

Close inspection (e.g. Fig. 3*A*) also shows that currents through sodium channels are followed by delayed outward currents, presumably through voltage-dependent potassium channels of the delayed-rectifier type. These currents are smaller than those recorded from frog skeletal muscle (e.g. Almers *et al.* 1983*a*) and are discussed later.

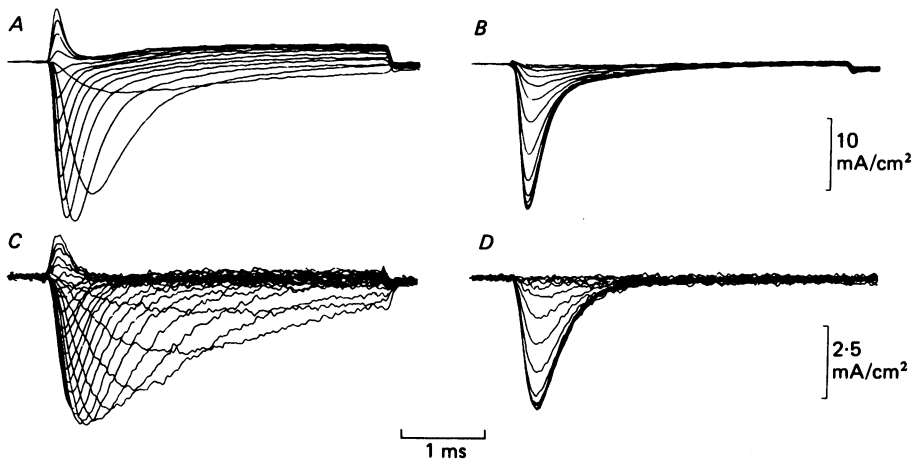

Fig. 3. Membrane currents from two fibres, from different biopsies, recorded after removal of slow inactivation (see text). *A* and *B*: fibre H-17; holding potential across patch membrane, h.p. = −103 mV; R_{is} = 0·71 MΩ; R_{os} = 0·25 MΩ. *C* and *D*: fibre H-4; patch holding potential −93 mV; R_{is} = 1·14 MΩ; R_{os} = 0·45 MΩ. *A*, currents during test depolarizations lasting 4 ms and varying in amplitude between 50 and 180 mV in steps of 10 mV. *C*, as in *A* but varying between 45 and 160 mV in steps of 5 mV. *B*, currents during a test depolarization to −13 mV, following 100 ms conditioning depolarizations to between −143 and −43 mV in 5 mV steps. *D*, as in *B* but test pulse to −8 mV following conditioning pulses to between −113 and −33 mV in 5 mV steps.

Determination of absolute membrane potential

Because the loose-patch technique relies entirely on extracellular measurements, it operates on a scale of potentials (denoted by the letter V) relative to the resting potential. The absolute transmembrane potential of the patch (denoted by E) was not known until the resting potential, E_0, was measured with an intracellular electrode. The two voltage scales were then related by $E = V + E_0$. In our experiments insertion of micro-electrodes caused the membrane potential to decline, but the pre-impalement potential could be calculated from other electrical parameters.

As in other excitable cells, sodium currents in human muscle are diminished ('inactivated') by depolarizing prepulses. Fig. 3*B* and *D* show superimposed traces during test pulses to a fixed potential preceded by prepulses of varying amplitudes. As the potential during prepulses becomes more positive, sodium current during the subsequent test pulse diminishes and ultimately disappears. The relationship between

peak sodium current and patch membrane potentials during prepulse is shown in Fig. 5*A* (circles) for the two fibres of Fig. 3. The prepulse potentials which inactivated half of the sodium current were: $V_h = -2$ mV (Fig. 3*B*) and $V_h = -14$ mV (Fig. 3*D*).

After the records in Fig. 3 were taken, E_0 was measured by inserting a fine glass micropipette into each of the two fibres at a distance of between 100 and 150 μm from the patch recording site. After impalement, E_0 at first changed rapidly and then within the next ~ 60 s reached a steady and less negative value (-57 mV for the fibre of Fig. 3*A* and *B* and -48 mV for that of Fig. 3*C* and *B*). When the measurements in Fig. 3*B* and *D* were repeated, with 5 and 10 min having elapsed between the first and second series of records, V_h was found to be -18 mV and -24 mV, respectively. Since micro-electrode impalement is unlikely to change the inactivation parameter so quickly, we attribute the observed change to the decline in resting potential, and we conclude that the patch records in Fig. 3*A* and *B* were obtained with an internal resting potential of $E_0 = (-57+2-18)\,\text{mV} = -73$ mV, and those of Fig. 3*C* and *D* with E_0 of $(-48+14-24) = -58$ mV.

Other electrical parameters also became more negative with respect to the resting potential. For the fibre of Fig. 3*C* and *D* the difference between resting potential (E_0) and reversal potential ($\bar{E}_{Na}$), namely $\bar{V}_{Na}$, changed from 99 mV to 80 mV, a 19 mV change. We also plotted peak sodium conductance, G_{Na}, against potential (not shown), where

$$G_{Na} = I_{Na}/(V - \bar{V}_{Na}), \tag{1}$$

and where I_{Na} is the peak sodium current at the potential V. The potential where G_{Na} was half-maximal, called the 'half-activation potential', V_G, also became more negative. Once again these changes most probably occurred because the resting potential became more positive following micro-electrode insertion. In five fibres, all three parameters – V_h, $\bar{V}_{Na}$ and V_G – were measured before and after impalement. Compared with pre-impalement potentials calculated from changes in V_h, those calculated from changes in $\bar{V}_{Na}$ were $2{\cdot}6 \pm 2{\cdot}0$ mV more negative, and those from changes in V_G were $1{\cdot}5 \pm 1{\cdot}4$ mV more positive; values are given $\pm$S.E. of mean. These differences are small or insignificant, therefore all three methods give closely similar results. In the remainder, the change in V_h was used to calculate E_0 before impalement, because V_h could be measured with greater accuracy.

Gating of sodium channels

Membrane currents and other electrical parameters can now be referred to E, the potential across the membrane patch. Fig. 4 plots peak currents through the Na channel against E. Reversal potentials, $\bar{E}_{Na}$, are 42 and 41 mV for the two fibres. Fig. 5*A* plots peak sodium current during fixed test steps to -10 or 0 mV against the potential during a conditioning prepulse (left). Values are given as a fraction of those obtained with hyperpolarizing prepulses. The points trace out the familiar 'h_∞ curve' (Hodgkin & Huxley, 1952) and describe the steady-state dependence of inactivation on potential. The line is a least squares fit of the equation

$$h_\infty = \frac{1}{1+\exp[(E-E_h)/k_h]}, \tag{2}$$

to the data in Fig. 3*B*. E is the transmembrane potential during the prepulse, E_h is the value where sodium currents are half-maximal, and k_h is a parameter determining how steeply h_∞ depends on membrane potential.

In order to describe the voltage dependence of activation, one could plot peak sodium conductance against potential, with peak sodium conductance calculated by an equation similar to eqn. (1). When this is done, peak conductance is found to rise with depolarization, to reach a maximum at around $E = -10$ mV and decline again at more positive potentials (not shown). Such a decline is expected because the conductance of a single sodium channel is known to diminish at positive potentials (e.g. Sigworth, 1977), presumably because the concentration of the most permeant ion, sodium, is less inside the cell than outside. The usual way to correct for this

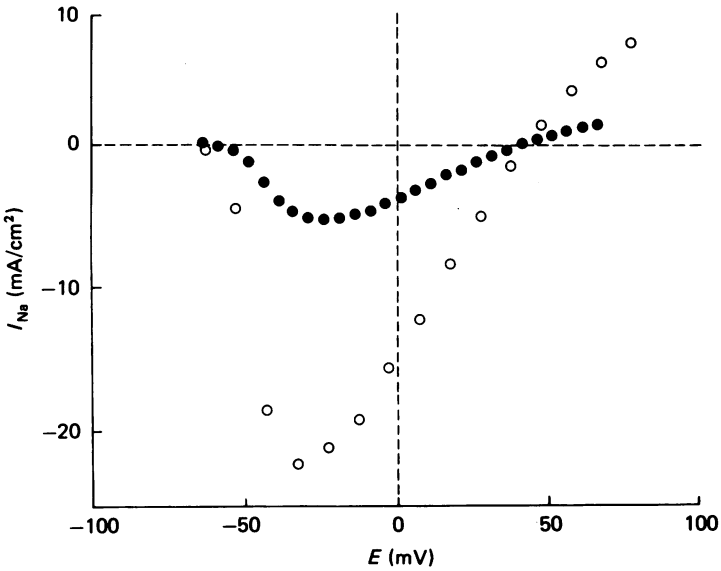

Fig. 4. Peak currents through sodium channels plotted against patch membrane potential. Same experiments as in Fig. 3 and 5. ○, fibre H-17; ●, fibre H-4.

asymmetric ion distribution is to consider instead the sodium permeability, P_{Na} (Hodgkin & Katz, 1949; Frankenhaeuser, 1960):

$$P_{Na} = \frac{I_{Na}}{F[Na]_o} \frac{kT}{E} \frac{\exp(E/kT)-1}{\exp[(E-\tilde{E}_{Na})/kT]-1}. \quad (3)$$

Here F is Faraday's constant; $[Na]_o$ is the sodium concentration in the bath; and $kT \simeq 26$ mV at 23 °C, being the product of Boltzmann's constant and absolute temperature. Peak P_{Na} as a fraction of the maximum value is plotted against potential in Fig. 5*B*. At around −60 to −50 mV P_{Na} rises steeply with depolarization (e-fold in 4·5 mV for the experiment of Fig. 3*C*) reaching a maximum at moderately positive potentials. At large potentials, P_{Na} declines again, though less markedly than G_{Na} (not shown). This was observed in all fibres studied. A similar result was also obtained on rat muscle by Pappone (1980). One may suggest that the number of open channels during peak current diminishes at extremely positive potentials. More likely, a single sodium channel does not obey the constant-field equation, and its 'permeability' as defined by eqn. (3) declines at positive potentials.

In an attempt to describe the kinetics of sodium channel activation, the time needed for sodium current to reach half its maximum was measured at each potential. We subtracted 48 μs from all values to allow for the delay introduced by our Bessel filter (see Methods). The result, $t_{\frac{1}{2}}$, rapidly declines to values < 100 μs. In a squid axon at

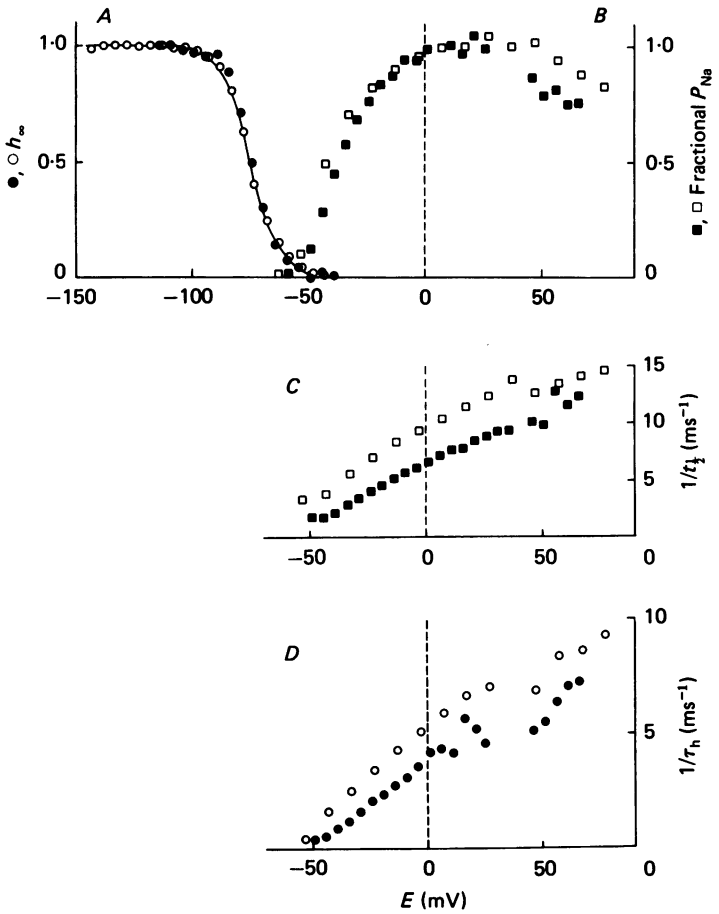

Fig. 5. Gating parameters for sodium channels. Results were obtained from the experiments in Fig. 3. Open symbols, fibre H-17 (Fig. 3*A* and *B*); filled symbols, fibre H-4 (Fig. 3*C* and *D*). *A*, dependence of peak sodium current on the potential during a conditioning prepulse (inactivation). The curve was drawn using eqn. (2) with $E_h = -75$ mV, $k_h = 6{\cdot}2$ mV, and is the best least squares fit to the open circles. *B*, dependence of peak sodium permeability on potential. Permeabilities were normalized to the maximum value observed, namely 3·8 μm/s (■) and 14·3 μm/s (□). *C*, kinetics of activation. Ordinate, reciprocal of time needed for current to increase to half its maximum value. *D*, potential dependence of inactivation kinetics. Ordinate, reciprocal time constant of current decline. *B*, *C*, *D* were derived from fig. 3*A* and *C*; *A* was derived from Fig. 3*B* and *D*.

6 °C, $t_{\frac{1}{2}}$ would correspond to $\sim 1{\cdot}1\ \tau_m$, where τ_m is the time constant of Hodgkin & Huxley's (1952) activation parameter, m. The correspondence is approximate, and the proportionality factor between the two variables is weakly voltage dependent. Fig. 5*C* plots $1/t_{\frac{1}{2}}$ against potential. The rate of sodium channel activation rises

approximately linearly with potential over the entire voltage range examined, as in frog (Campbell & Hille, 1976) and rat muscle (Pappone, 1980) and also in squid axons (Hodgkin & Huxley, 1952).

Fig. 5*D* describes the potential dependence of the rate at which sodium channels inactivate. Exponentials were fitted to the decline of currents through sodium channels, and the reciprocal of their time constants are plotted in Fig. 5*D*. Time constants decrease about twentyfold as potentials range from −50 to +60 mV. In other preparations (squid axon: Armstrong & Bezanilla, 1977; frog muscle: Hille & Campbell, 1976; rat muscle: Pappone, 1980) time constants appear to approach asymptotically a minimum value at extreme positive potentials, as though a

TABLE 1. Membrane currents in human muscle

Fibre no.	H-2	H-4	H-5	H-12	H-13	H-17	Mean ± S.E. of mean	
E_0 (mV)	−48	−58	−64	−67	−68	−73	−63	3·6
h.p. (mV)	−108	−93	−104	−107	−88	−103	−101	3·3
$\bar{G}_{Na}$ (mS/cm²)	187	95	44	181	110	360	163	45
$\bar{P}_{Na}$ (μm/s)	7·1	3·8	1·3	6·3	4·7	14·3	6·3	1·8
$\bar{I}_{Na}$ (mA/cm²)	−11	−5	−2	−12	−8	−22	−10·0	2·8
$\bar{E}_{Na}$ (mV)	44	41	29	39	43	42	40	2·3
E_G (mV)	−45	−39	−52	−53	−43	−45	−46	2·2
E_P (mV)	−41	−34	−53	−50	−38	−41	−43	3·0
E_h (mV)	−90	−72	−111	−89	−81	−75	−86	5·8
k_h (mV)	5·8	5·5	6·4	5·3	6·1	6·2	5·9	0·2
$\bar{G}_K$ (mS/cm²)	4·0	2·6	0·0	9·1	13·0	18·6	7·9	2·9

E_0, resting potential corrected for micro-electrode impalement damage by comparing V_h before and after impalement (see text). h.p. holding potential across the patch membrane. $\bar{I}_{Na}$, $\bar{G}_{Na}$ and $\bar{P}_{Na}$, maximal values of sodium current, sodium conductance (eqn. 1) and sodium permeability (eqn. 3) recorded in each fibre. $\bar{E}_{Na}$, sodium channel reversal potential. E_G and E_P, potentials where $G_{Na} = 0{\cdot}5\ \bar{G}_{Na}$ and where $P_{Na} = 0{\cdot}5\ \bar{P}_{Na}$, respectively. E_h, potential where half the sodium channels are inactivated by a 100 ms prepulse. k_h determines how steeply h_∞ depends on potential and is defined by eqn. (2). G_K, maximal potassium conductance, as defined in Fig. 6.

potential-independent step ultimately becomes rate limiting for inactivation. Such a step would be the entry of an endogenous intracellular blocking particle into the open channel (Armstrong & Bezanilla, 1977; Cahalan & Almers, 1979). In Fig. 5*D* any such asymptotic behaviour is obscured by scatter; however, averaged results in Fig. 8*C* suggest that time constants tend towards a limiting value of about 0·12–0·14 ms at 23 °C.

Table 1 summarizes data from experiments as in Figs. 3–5, including data from six fibres from four patients. All entries refer to measurements made before micro-electrode insertion. Some parameters showed little variation from fibre to fibre, such as the reversal potential $\bar{E}_{Na}$, the potentials for half-maximal conductance (E_G) and permeability (E_P), and the voltage sensitivity of inactivation (k_h). The mid-point of the h_∞ curve varied more markedly, with fibre showing values that, if applicable *in vivo*, would render more than half of the sodium channels inactive at the resting potential. The maximal sodium conductance or permeability, presumably a measure of sodium channel density in the patch, showed the largest variation.

Data also were obtained from eight other fibres from the same set of biopsies. In these experiments, V_h was not measured after electrode insertion, and therefore the resting potential was less certain. The following values, given $\pm$S.E. of mean, are not expected to depend strongly on the resting potential: $\tilde{G}_{Na} = 124 \pm 27$ mS/cm^2, $\tilde{P}_{Na} = 5{\cdot}3 \pm 1{\cdot}4$ μm/s, $k_h = 5{\cdot}6 \pm 0{\cdot}3$ mV. V_G was somewhat more positive, and V_{Na} considerably more positive in these fibres. If we assume that the potential for half-maximal activation of conductance (E_G) has a constant value of -46 mV (Table 1) and use this value to calculate resting potentials, we obtain: $E_0 = -73 \pm 5$ mV; $E_h = -85 \pm 2$ mV, $E_{Na} = 47 \pm 3$ mV. These values agree well with those of Table 1, except that the resting potential is more negative and the reversal potential more positive.

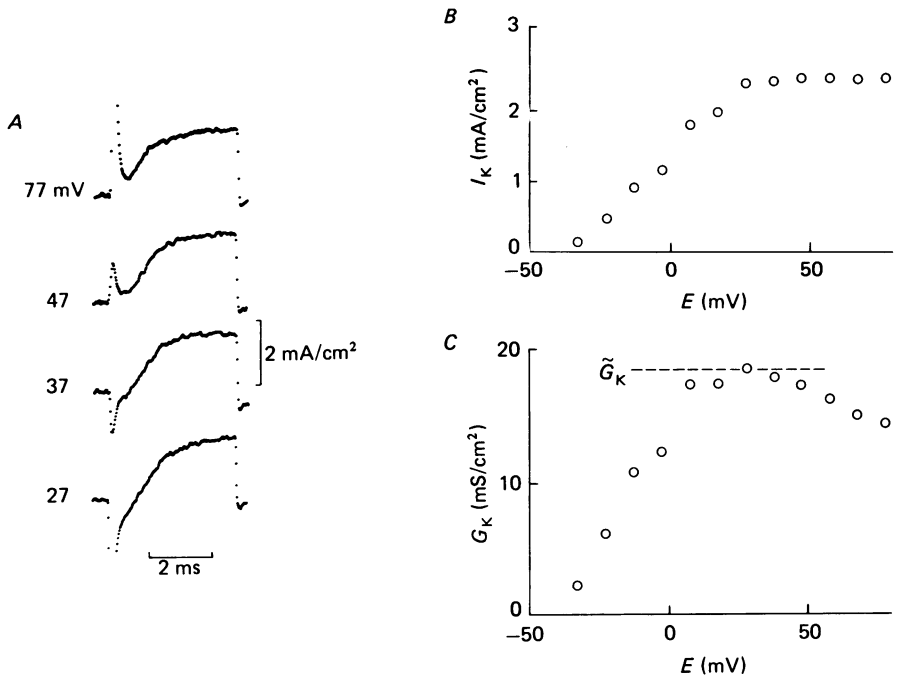

Fig. 6. *A*, currents during potential steps from -103 mV to the potential indicated next to each trace. Traces were selected from Fig. 3*A* and are shown at a higher gain. Currents through sodium channels are off scale at 77 and 27 mV. *B*, ΔI. *C*, G_K plotted against potential, where ΔI and G_K are defined in eqn. (4).

Potassium currents

Throughout, potassium currents were small relative to sodium currents or relative to delayed potassium currents in frog muscle (Almers *et al.* 1983*a*). Fig. 6*A* shows some of the traces of Fig. 3*A* at higher gain; the large currents through the sodium channel are mostly off scale. At the most positive potentials an increase in potential does not lead to an increase in current (Fig. 6*B*). In Fig. 6*C* the final conductance, G_K, is plotted against potential. G_K was calculated as

$$G_K = \frac{\Delta I}{\Delta E}, \tag{4}$$

where ΔI and ΔE are current and voltage changes at the moment of repolarization. It is seen that G_K declines at extreme positive potentials. This was generally not observed in loose-patch clamp experiments on frog skeletal muscle (Almers *et al.* 1983*a*; W. M. Roberts, unpublished), but was seen consistently in the present experiments. The effect cannot be due to cumulative inactivation, as test pulses were applied in order of decreasing amplitudes throughout this work. In these fibres the largest conductance ($\tilde{G}_K$) was usually observed between 10 and 30 mV. $\tilde{G}_K$ varied widely from patch to patch (range 0–22 mS/cm²) and the average value was $6{\cdot}6 \pm 1{\cdot}4$ mS/cm² (±S.E. of mean, $n = 14$). $\tilde{G}_K$ and $\tilde{G}_{Na}$ were weakly correlated, with a correlation coefficient of $r = 0{\cdot}70$ in fourteen fibres.

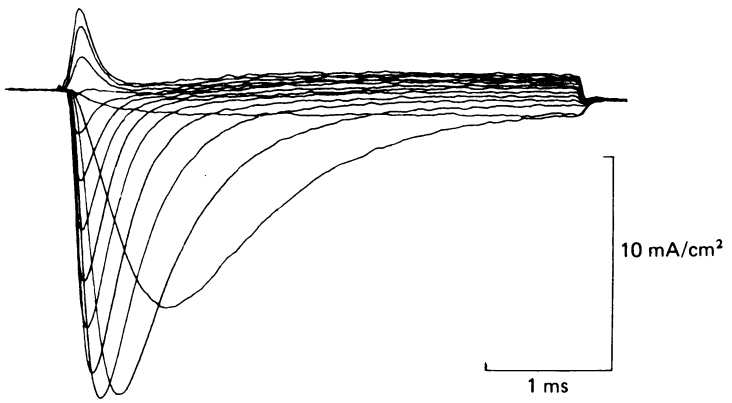

Fig. 7. Membrane currents in rat omohyoid muscle. Holding potential across patch membrane, h.p. = −93 mV. Currents were in response to steps varying in amplitude between 30 and 160 mV in increments of 10 mV. Fibre R-6; resting potential = −63 mV; $R_{is} = 0{\cdot}67$ MΩ; $R_{os} = 0{\cdot}38$ MΩ.

Measurements on rat omohyoid muscle

Resting membrane potentials appeared more stable in rat than in human muscle. This may be due entirely to mechanical factors favouring micro-electrode impalement; the rat omohyoid muscle is a flat and compact muscle that allowed good visibility and mechanical support in our experimental chamber, whereas the fascicles dissected from human intercostal muscle were loose and more rounded in shape. Since resting potentials in rat were so stable, we took the measured values to apply also to pre-impalement recordings of membrane currents. As in human muscle, currents were greatly increased in size by ~ 10 min of hyperpolarization of the patch by 20–30 mV.

The membrane currents in Fig. 7 were obtained approximately 10 min after applying a holding potential of −93 mV. They appear closely similar to those in Fig. 3*A* and *C* and consist of an early transient current reversing direction at 39 mV and a smaller delayed outward current. Maximal inward current ($\tilde{I}_{Na}$) varied widely, ranging from −5 to −17 mA/cm² in five fibres. Inactivation of the early (sodium) current was investigated as in Fig. 3*B* and *D* (not shown), and the voltage dependences of P_{Na}, τ_h and $t_{\frac{1}{2}}$ were analysed as in Fig. 5. Averages of results on five

fibres are presented in Table 2 and Fig. 8 (open symbols) along with average results from human intercostal muscle. In Table 2 the results from rat muscle appear similar or identical to those on human muscle in all features, with one possible exception: in rat, the potential where $h_\infty = 0{\cdot}5$ was less negative with respect to the resting potential. In rat, $V_h = -5{\cdot}0 \pm 6{\cdot}2$ mV ($n = 6$), whereas in human fibres $V_h = -19{\cdot}9 \pm 4{\cdot}6$ mV ($n = 17$); values are given ±S.E. of mean and include results on fibres where the resting potential was not accurately known. This difference is at least partly due to the fact that E_h was more positive in our rat than in our human results (Table 2). This may reflect a healthier physiological state of our rat omohyoid muscles.

TABLE 2. Comparison between human and rat skeletal muscle

	Human	n	Rat	n
E_0 (mV)	$-63 \pm 3{\cdot}6$	6	-68 ± 4	5
$\bar{G}_{Na}$ (mS/cm²)	140 ± 24	14	195 ± 29	5
$\bar{P}_{Na}$ (μm/s)	$5{\cdot}7 \pm 1{\cdot}1$	14	$7{\cdot}8 \pm 1{\cdot}0$	5
$\bar{I}_{Na}$ (mA/cm²)	$-9{\cdot}4 \pm 1{\cdot}7$	14	$-12 \pm 4{\cdot}9$	5
$\bar{E}_{Na}$ (mV)	$40 \pm 2{\cdot}3$	6	42 ± 1	5
E_G (mV)	$-46 \pm 2{\cdot}2$	6	-46 ± 4	5
E_P (mV)	$-43 \pm 3{\cdot}0$	6	-40 ± 4	5
E_h (mV)	-86 ± 6	6	-76 ± 5	5
k_h (mV)	$5{\cdot}7 \pm 0{\cdot}2$	14	$5{\cdot}7 \pm 0{\cdot}2$	5
$\bar{G}_K$ (mS/cm²)	$6{\cdot}6 \pm 1{\cdot}4$	14	$7{\cdot}9 \pm 1{\cdot}3$	5

Symbols have the same significance as in Table 1. Where $n = 6$ for human muscle, values were taken from Table 1; where $n = 14$, values include those in Table 1 as well as others where the membrane potential is not known with precision. Values are given ±S.E. of mean.

Fig. 8 summarizes our analysis of kinetics and voltage dependence of sodium current in rat and human muscle. For each fibre, data points as in Fig. 5*B*, *C* and *D* were connected by straight lines, so that values at potentials differing from 0 mV by 10 mV increments could be obtained by interpolation. These values were then averaged for all fibres. Data obtained within ±10 mV of the reversal potential were rejected as too inaccurate, so the points in that potential range are the result of interpolation over a 20–30 mV interval. Fig. 8*A* and *C* show that rates of sodium current activation ($1/t_{\frac{1}{2}}$) and inactivation ($1/\tau_h$) are similar for rat (open symbols) and human muscle (filled symbols); what differences exist may be due to experimental uncertainties, such as slight differences in temperature, or in inaccuracy of data at the most positive potentials.

The plots of normalized peak permeability against potential (Fig. 8*B*) were obtained in a slightly different manner. Curves as in Fig. 5*B* were aligned by shifts along the voltage axis, so that the potentials for half-maximal permeability superimposed at $E_P = -43$ mV for all human curves and at $E_P = -40$ mV for all rat curves. These potentials were chosen because they are the averages for half-maximal sodium permeability in man and rat, respectively (see Table 2). Points at potentials differing from E_P in 10 mV increments then were obtained by interpolation as before; data within ±10 mV of the reversal potential were rejected. The aim of aligning curves to coincide at −43 mV and −40 mV was to ensure that the steep

voltage dependence of P_{Na} observed in each individual fibre was not lost in the averaging process. Once again, data for rat and human muscle appear closely similar or identical; the small difference in E_P could easily be due to experimental uncertainty.

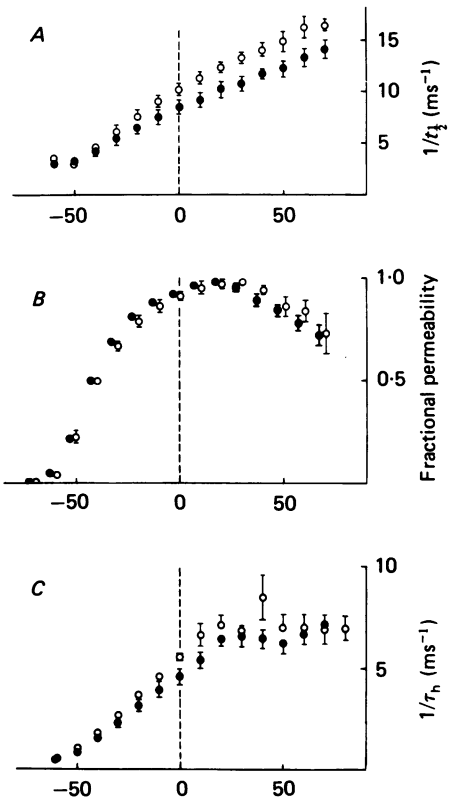

Fig. 8. Comparison of sodium channel gating parameters in rat omohyoid (open symbols) and human intercostal muscle (filled symbols). Human data are averages from the six fibres of Table 1, rat data are averages from the five fibres of Table 2. Error bars indicating S.E. of mean are shown if they exceed the size of the symbol. For details see text.

Late outward (potassium) currents in rat muscle were relatively small; as in human muscle, their amplitude saturated at positive potentials, indicating a decline of potassium conductance. G_K was maximal at 10–40 mV and varied widely from fibre to fibre ($\bar{G}_K$ = 4–12 mS/cm^2), with the average value being similar to that found in human muscle.

DISCUSSION

This paper shows that the 'loose-patch' voltage clamp method (Almers *et al.* 1983*a*; Stühmer *et al.* 1983) can be used to record membrane currents from fibres contained in whole muscles or muscle fascicles of rats and humans. For the present work, the

main advantage of the loose-patch technique is that it requires less disturbance of the tissue than any other presently available voltage-clamp method. A disadvantage in earlier loose-patch experiments was contamination of experimental records by uncontrolled currents across the sarcolemma beneath the pipette rim (Almers *et al.* 1983*a*, their fig. 5). In the present work this problem was avoided by using concentric pipettes, and by collecting currents only from the central portion of a larger, isopotential patch.

Comparison with previous work on rat muscle

Membrane currents in rat skeletal muscle have been recorded from cut fibres of sternomastoid and extensor digitorum longus (e.d.l.) with the Vaseline-gap method (Pappone, 1980), from intact fibres of iliacus and soleus muscles with the sucrose-gap method (Duval & Léoty, 1978, 1980) and from osmotically shrunken but otherwise intact fibres of e.d.l. with a method using three micro-electrodes (Adrian & Marshall, 1977).

Most of our results agree well with the earlier data. The *reversal potential*, E_{Na}, is given as 47·9 mV (iliacus) and 41·3 mV (soleus) by Duval & Léoty (1980); our value for the omohyoid is 42 mV. Our value for the maximal potassium conductance ($\bar{G}_K = 7{\cdot}9$ mS/cm^2) agrees with that of Pappone (1980). She gives a value of $\bar{G}_K = 12$ mS/cm^2 at 20 °C for a group of four fibres, noting that she saw no potassium currents in other fibres. Beam & Donaldson (1983) report a higher value of 22 mS/cm^2 at 21–23 °C; however, their measurements were made in hypertonic solution where internal potassium concentration may have been 2–2·5 times normal. For frog muscle, an average value of $\bar{G}_K = 5{\cdot}7$ mS/cm^2 has been found at the ends of sartorius fibres (Almers, 1976, 5 °C); in hypertonic solutions, higher values are found (18 mS/cm^2; Stanfield, 1975). However, potassium currents in frog are highly variable. In the middle of muscle fibres, values of 5–10 mA/cm^2 are frequently seen with 120–130 mV steps (Almers *et al.* 1983*a*; see also Vaseline-gap measurements by Blatz, 1982), suggesting a conductance of 40–80 mS/cm^2.

To the extent that a comparison can be made, there is also reasonable agreement between the *gating parameters for sodium channels* found here and in the earlier work. In intact fibres the potential where peak sodium permeability is half-maximal was found to be about −45 mV (Adrian & Marshall, 1977, their fig. 6) or about −43 mV (Duval & Léoty, 1980, their fig. 4); our average value is −40 mV. The potential E_h where $h_\infty = \frac{1}{2}$ is given as −70 mV by Adrian & Marshall (1977, one fibre), as −73 mV by Duval & Léoty (1978), and as −63 mV (soleus) or −67 mV (iliacus) in a later paper by Duval & Léoty (1980). Our value is −76 mV, with considerable variation from fibre to fibre. Single-barrel loose-patch experiments by W. Stühmer, P. R. Stanfield & W. Almers (unpublished) gave an identical value of -77 ± 4 mV in fibres with an average resting potential of -69 ± 3 mV (values given are ± S.E. of mean, $n = 10$). Time constants of inactivation at 20 °C are given as about 2·2 ms at −57 mV, 0·4 ms at −13 mV, and about 0·22 ms at 43 mV by Pappone (1980); the corresponding values in Fig. 8 are 2·3 ms at −60 mV, 0·22 ms at −10 mV and 0·14 ms at 50 mV, all at 23 °C.

The only possible difference between our own and earlier measurements concerns the size of sodium currents. For a given fibre, the maximal value of I_{Na} had a mean

value of 11 mA/cm² in the present work; this is 2–3 times larger than found by Pappone (1980). We found sodium current amplitudes extremely variable from fibre to fibre. If sodium currents have a patchy distribution in rat, as they do in frog muscle (Almers *et al.* 1983*a*), it is possible that our loose-patch results are statistically biased towards larger sodium currents, as patches with small currents were more likely to be abandoned by the experimenter. However, our value of $\bar{G}_{Na} \simeq 200$ mS/cm² is consistent with measurements of saxitoxin binding (535 sites/μm² in e.d.l.: Hansen-Bay & Strichartz, 1980; 209 sites/μm² in diaphragm: Ritchie & Rogart, 1977) and single-channel conductance (18 pS: Sigworth & Neher, 1980). If half the sodium channels are open at the time of peak current (Sigworth, 1978) then our mean value of $\bar{G}_{Na} = 200$ mS/cm² would translate into a mean channel density of 200/μm², no higher than observed with saxitoxin binding.

Membrane currents in human muscle fibres

Previous attempts to record sodium currents have been made by Lehmann-Horn *et al.* (1983), who used micro-electrodes in the middle of an intact fibre, and also by De Coursey *et al.* (1982), who used a Vaseline-gap at 12 °C. This paper reports the first systematic investigation on intact fibres. Results from human and rat muscle are remarkably similar in almost all details (see Table 2 and Fig. 8).

The reversal potential of the sodium channel (mean 40 mV, range 29–44 mV) can be used to calculate the myoplasmic sodium concentration, $[Na]_i$. The ratio of potassium and sodium permeabilities is taken as $P_K/P_{Na} = 0{\cdot}05$ as in rat muscle (Pappone, 1980). The data of Ludin (1969) suggest that when the product of the external potassium and chloride concentrations, $[K]_o \times [Cl]_o$ is kept constant, the resting membrane potential of human intercostal muscle would be zero at $[K]_o = 156$ mM. Therefore we take the electrically effective myoplasmic concentration, $[K]_i$, as being 156 mM. With these values, one can calculate an average value of $[Na]_i$ of 24 mM (range 19–40 mM) by the familiar equation

$$\bar{E}_{Na} = kT \ln \frac{A[K]_o + [Na]_o}{A[K]_i + [Na]_i},$$

where $A = P_K/P_{Na}$. The value 24 mM is the same as that obtained on rat soleus muscle (24 mM: Akaike, 1976) and lower than the 59 mM obtained by chemical analysis of human intercostal muscle by Lipicky, Bryant & Salmon (1971). Lipicky *et al.* (1971) also give a higher value for $[K]_i$ (180 mM) than the one assumed here.

Potassium outward currents are variable and remarkably small compared with sodium currents, as is the case in rat muscle. Potassium currents are small or absent also in rabbit myelinated nerve (Chiu, Ritchie, Rogart & Stagg, 1979) and this may be characteristic of mammalian excitable tissues. In human muscles, G_K may need to be small in order to minimize the elevation of plasma potassium levels following exercise.

In both rat and human muscle, potassium current saturates at positive potentials. Such saturation was not observed in loose-patch recordings on frog muscle using concentric pipettes (W. M. Roberts, unpublished), and is therefore unlikely to be a consequence of the method. French & Wells (1977) observed saturation of I_K in squid

giant axons when sodium was present internally. With $[Na]_i = 25$ mM, they observed saturation between 100 and 200 mV. In our work the I_K/V curve became flat by 50 mV. While it is attractive to attribute saturation to internal sodium, the effect may have entirely different causes.

Both potassium and sodium currents were extremely variable in size. A patchy distribution of sodium and potassium channels was observed in frog muscle (Almers *et al.* 1983*a*) and may account for some of the variability observed.

Physiological state of human muscle fibres

Though experimental conditions were probably more physiological in this work than in most other voltage-clamp studies of mammalian muscle, we clearly fell short of simulating conditions *in vivo* in some respects. The most obvious is the lower temperature (23 °C as compared with 36–37 °C), and this should have consequences for the kinetics of ionic currents and for all electrical parameters that depend on cell metabolism. For example, the sodium/potassium pump may be somewhat inhibited, so that *in vivo* $[Na]_i$ may be lower and E_{Na} more positive. A lower $[Na]_i$ could, in principle, also allow greater values for $\bar{G}_K$; though on the basis of French & Wells' (1977) work on squid axons, any such effect is unlikely to matter at the potentials reached during an impulse.

Most or all of our fibres were inexcitable until excitability was locally restored by hyperpolarization. This was in part a direct consequence of low resting potentials, which are known to lead to inactivation of sodium channels. Resting potentials in this work (average −63 mV at 23 °C) were less negative than is found at 37 °C, both *in vivo* (−78 mV: Goodgold & Eberstein, 1966; −87 mV: Bolte, Riecker & Röhl, 1963) and *in vitro* (−80 mV: Ludin, 1969). However, depolarization may not have been the only reason for lack of excitability. The average mid-point of our h_∞ curve was at $E_h = -86$ mV, a potential which is probably more negative than E_h *in vivo*. The value of E_h was highly variable in our experiments, possibly reflecting a wide spectrum of physiologic states.

Despite these shortcomings, it seems clear than an improved loose-patch method is a convenient tool for studying muscle membrane excitability under nearly physiological conditions. Though it may be difficult to study sodium currents at 37 °C with this or any other voltage-clamp technique, careful attention to dissection and maintenance of our preparation should produce more physiological values for resting potentials in E_h in future experiments. It seems likely that the method will allow collection of complete data on the major conductance systems involved in excitation of human muscle. Such data could serve as a reference for future biophysical studies of muscle disease.

We thank Dr R. Valdiosera for help with some of these experiments, Drs J. Weeks and W. Stühmer for helpful criticisms, and L. Miller for expert preparation of the manuscript. R. L. R. was the recipient of an N.I.H. Teacher Investigator Award (no. NS00498). Supported by U.S.P.H.S. grant no. NS18748.

REFERENCES

ADRIAN, R. H., CHANDLER, W. K. & HODGKIN, A. L. (1970). Voltage clamp experiments in striated muscle fibres. *J. Physiol.* **208**, 607–644.

ADRIAN, R. H. & MARSHALL, M. W. (1977). Sodium currents in mammalian muscle. *J. Physiol.* **268**, 223–250.

AKAIKE, N. (1976). Intracellular ion concentration and electrical activity in potassium-depeleted mammalian soleus muscle fibers. *Pflügers Arch.* **362**, 15–20.

ALMERS, W. (1976). Differential effects of tetracaine on delayed potassium channels and displacement currents in frog skeletal muscle. *J. Physiol.* **262**, 613–637.

ALMERS, W., STANFIELD, P. R. & STÜHMER, W. (1983*a*). Lateral distribution of sodium and potassium channels in frog skeletal muscle: measurements with a patch-clamp technique. *J. Physiol.* **336**, 261–284.

ALMERS, W., STANFIELD, P. R. & STÜHMER, W. (1983*b*). Slow changes in currents through sodium channels in frog muscle membrane, *J. Physiol.* **339**, 253–271.

ARMSTRONG, C. M. & BEZANILLA, F. (1977). Inactivation of the sodium channel. II. Gating current experiments. *J. gen. Physiol.* **70**, 567–590.

BEAM, K. G. & DONALDSON, P. L. (1983). A quantitative study of potassium channel kinetics in rat skeletal muscle from 1 to 37 °C. *J. gen. Physiol.* **81**, 485–512.

BLATZ, A. L. (1982). Modification of potassium channels in skeletal muscle by low pH and chemical modifiers. Ph.D. thesis, University of Washington, Seattle.

BOLTE, H. D., RIECKER, G. & RÖHL, D. (1963). Messungen des Membranpotentials an einzelnen quergestreiften Muskelzellen des Menschen *in situ*. *Klin. Wochenschr.* **41**, 356–359.

CAHALAN, M. D. & ALMERS, W. (1979). Block of sodium conductance and gating current in squid giant axons poisoned with quaternary strychnine. *Biophys. J.* **27**, 57–74.

CAMPBELL, D. T. & HILLE, B. (1976). Kinetic and pharmacological properties of the sodium channel of frog skeletal muscle. *J. gen. Physiol.* **67**, 309–323.

CHIU, S. Y., RITCHIE, J. M., ROGART, R. B. & STAGG, D. (1979). A quantitative description of membrane currents in rabbit myelinated nerve. *J. Physiol.* **292**, 149–166.

DE COURSEY, T. E., BRYANT, S. H. & LIPICKY, R. J. (1982). Sodium currents in human skeletal muscle fibers. *Muscle and Nerve* **5**, 614–618.

DUVAL, A. & LÉOTY, C. (1978). Ionic currents in mammalian fast skeletal muscle. *J. Physiol.* **278**, 403–423.

DUVAL, A. & LÉOTY, C. (1980). Ionic currents in slow twitch skeletal muscle in the rat. *J. Physiol.* **307**, 23–41.

FRANKENHAEUSER, B. (1960). Quantitative description of sodium currents in myelinated nerve fibres of *Xenopus laevis*. *J. Physiol.* **151**, 491–501.

FRENCH, R. J. & WELLS, J. B. (1977). Sodium ions as blocking agents and charge carriers in the potassium channel of the squid giant axon. *J. gen. Physiol.* **70**, 707–724.

GOODGOLD, J. & EBERSTEIN, A. (1966). Transmembrane potentials in human muscle cells *in vivo*. *Expl Neurol.* **15**, 338–346.

HANSEN-BAY, C. & STRICHARTZ, G. R. (1980). Saxitoxin binding to sodium channels of rat skeletal muscle. *J. Physiol.* **300**, 89–103.

HENČEK, M., NONNER, W. & STÄMPFLI, R. (1969). Voltage clamp of a small muscle membrane area by means of a circular sucrose gap arrangement. *Pflügers Arch.* **313**, 71–79.

HILLE, B. & CAMPBELL, D. T. (1976). An improved vaseline gap voltage clamp for skeletal muscle fibers. *J. gen. Physiol.* **67**, 265–293.

HODGKIN, A. L. & HUXLEY, A. F. (1952). A quantitative description of membrane current and its application to conduction and excitation in nerve. *J. Physiol.* **117**, 500–544.

HODGKIN, A. L. & KATZ, B. (1949). The effect of sodium ions on the electrical activity of the giant axon of the squid. *J. Physiol.* **108**, 37–77.

ILDEFONSE, M. & ROUGIER, O. (1972). Voltage-clamp analysis of the early current in frog skeletal muscle fibre using the double sucrose-gap method. *J. Physiol.* **222**, 373–395.

LEHMANN-HORN, F., RÜDEL, R., DENGLER, R., LORKOVIĆ, H., HAASS, A. & RICKER, K. (1981). Membrane defects in paramyotonia congenita with and without myotonia in a warm environment. *Muscle and Nerve* **4**, 396–406.

LEHMANN-HORN, F., RÜDEL, R., RICKER, K., LORKOVIĆ, H., DENGLER, R. & HOPF, H. C. (1983). Two cases of adynamia episodica hereditaria: *in vitro* investigation of muscle cell membrane and contraction parameters. *Muscle and Nerve* **6**, 113–121.

LIPICKY, R. J. & BRYANT, S. H. (1973). A biophysical study of the human myotonias. In *New Developments in Electromyography and Clinical Neurophysiology*, ed. DESMEDT, J. E., pp. 451–463. Basel: Karger.

LIPICKY, R. J., BRYANT, S. H. & SALMON, J. H. (1971). Cable parameters, sodium, potassium, chloride, and water content, and potassium efflux in isolated external intercostal muscle of normal volunteers and patients with myotonia congenita. *J. clin. Invest.* **50**, 2091–2103.

LUDIN, H. P. (1969). Microelectrode study of normal human skeletal muscle. *Eur. Neurol.* **2**, 340–347.

PAPPONE, P. A. (1980). Voltage-clamp experiments in normal and denervated mammalian skeletal muscle fibres. *J. Physiol.* **306**, 377–410.

RITCHIE, J. M. & ROGART, R. B. (1977). The binding of labelled saxitoxin to the sodium channels in normal and denervated mammalian muscle, and in amphibian muscle. *J. Physiol.* **269**, 341–354.

RUFF, R. L. & GORDON, A. M. (1984). Disorders of muscle: the periodic paralyses. In *The Physiology of Membrane Disorders*, ed. ANDREOLI, T. E., HOFFMAN, J. F., FANESTIL, D. P. & SCHULTZ, S. G., chap. 52. New York: Plenum Press (in the Press).

RUFF, R. L., MARTYN, D. & GORDON, A. M. (1982). Glucocorticoid-induced atrophy is not due to impaired excitability of rat muscle. *Am. J. Physiol.* **243**, E512–521.

SIGWORTH, F. J. (1977). Sodium channels in nerve apparently have two conductance states. *Nature, Lond.* **270**, 265–267.

SIGWORTH, F. J. (1978). Fraction of sodium channels open at peak conductance. *Biophys. J.* **21**, 41a.

SIGWORTH, F. J. & NEHER, E. (1980). Single Na^+ channel currents observed in cultured rat muscle cells. *Nature, Lond.* **287**, 447–449.

STANFIELD, P. R. (1975). The effect of zinc ions on the gating of the delayed potassium conductance of frog sartorius muscle. *J. Physiol.* **251**, 711–735.

STÜHMER, W. & ALMERS, W. (1982). Photobleaching through glass micropipettes: sodium channels without lateral mobility in the sarcolemma of frog skeletal muscle. *Proc. natn. Acad. Sci. U.S.A.* **79**, 946–950.

STÜHMER, W., ROBERTS, W. M. & ALMERS, W. (1983). The loose patch clamp. In *Single Channel Recording*, ed. SAKMANN, B. & NEHER, E. New York: Plenum Press (in the Press).

EXPLANATION OF PLATE

Photograph of one of the concentric-barrelled patch electrodes used in this work, viewed from a 45° angle. The centre barrel is nearly triangular in cross-section and protrudes slightly beyond the outer barrel tip. The three support tubes which maintain the separation between the centre and outer barrels were drawn into thin sheets during the pulling process and retracted when the tip was heat-polished. Calibration = 10 μm.